

## Study on Thermal Stress of Honeycomb Ceramic Regenerators with Different Parameters

Y. X. Wang,<sup>a</sup> M. Dong,<sup>a</sup> H. Y. Li,<sup>b</sup> Y. Q. Liu,<sup>a,1</sup> and Q. H. Shang<sup>a</sup>

<sup>a</sup> School of Traffic and Vehicle Engineering, Shandong University of Technology, Zibo, China

<sup>b</sup> School of Electrical & Electronic Engineering, Zibo Vocational Institute, Zibo, China

<sup>1</sup> liuyq65@163.com

УДК 539.4

## Исследование температурного напряжения керамического сотового регенератора с различными параметрами

Я. Ванг<sup>a</sup>, М. Донг<sup>a</sup>, Х. Г. Ли<sup>b</sup>, Й. К. Лиу<sup>a,1</sup>, К. Х. Шанг<sup>a</sup>

<sup>a</sup> Факультет проектирования дорог и транспортных средств, Шаньдунский университет технологий, Цзыбо, Китай

<sup>b</sup> Факультет электромашиностроения и электроники, Цзыбоский профессиональный институт, Цзыбо, Китай

*При работе ядерного реверс-поточного реактора керамические сотовые регенераторы подвергаются действию термоударной нагрузки. С помощью программного обеспечения CFX проведено численное моделирование эйор температуры и температурного напряжения керамических сотовых регенераторов. Исследовано изменение температур во времени для керамических сотовых регенераторов с отверстиями различной формы. Проанализированы эйоры температурного напряжения регенераторов с разными конструкционными и эксплуатационными параметрами. Установлено, что температурное напряжение керамического сотового регенератора зависит от формы отверстий, пористости и толщины стенок. Результаты данного исследования служат теоретической базой для оптимизации керамических сотовых регенераторов.*

**Ключевые слова:** керамический сотовый регенератор, численное моделирование, температура, температурное напряжение.

**Introduction.** Thermal flow-reversal reactor (TFRR) technology is an effective technology widely applied to greenhouse gas elimination and heat recovery from ventilation air methane (VAM) of coal mines [1–5]. This technology is based on flow-reversal principle. The heat of combustion is first transferred to a solid medium and then the incoming air, in order to raise its temperature to the ignition temperature of methane. The solid medium usually consists of a number of honeycomb ceramics. In TFRR operations, honeycomb ceramic regenerators are exposed to thermal shock load, making their thermal shock resistance very critical.

Domestic and foreign scholars who studied honeycomb ceramic regenerators mainly focused on the heat transfer characteristics [6, 7] and paid little attention to thermal shock resistance of them [8]. Nevertheless, thermal shock resistance is one of the main factors that control the service life of regenerators. Ou et al. [9] performed a numerical study on the stress variation pattern at the cellular hole wall surface of honeycomb ceramic regenerators, and found that frequent switching over between heat accumulation and release processes will subject the cellular hole wall to tension and extrusion stresses alternately. This finding

was also confirmed by later research [10]. Thermal shock capability of regenerators depends on internal thermal stress, which is influenced by the geometric structure and environmental media [11–13]. Relationship between the geometric properties of regenerators (holes, porosity and thickness) and thermal stress is studied in this paper.

**1. Temperature Distribution of Regenerators.**

**1.1. Geometric Parameters of Calculation Model.** A mullite regenerator was taken as the study object. Through numerical simulation, the temperature and thermal stress distributions of honeycomb ceramics were studied. Table 1 lists the structural parameters of the regenerators used in the paper. In order to establish a simplified mathematical model, widths and heights of the regenerators were reduced proportionally. Figure 1 shows the 3D physical model of a typical heat regenerator.

T a b l e 1

**Structural Parameters of Regenerators**

Serial number	Hole pattern	Wall thickness (mm)	Length (mm)	Porosity
1#	Square	0.7	3.0	0.64
2#	Square	1.0	3.1	0.57
3#	Square	1.0	2.5	0.51
4#	Hexagon	1.2	2.17	0.57
5#	Round	1.0	4.0	0.64
6#	Round	1.3	4.0	0.57
7#	Round	1.8	4.5	0.51

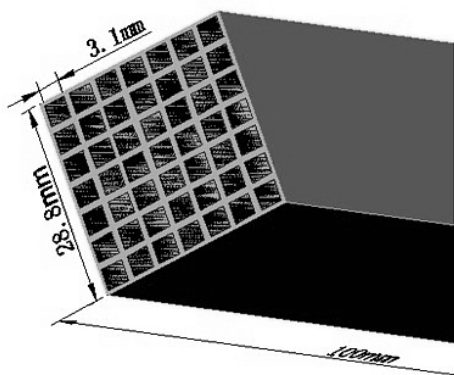


Fig. 1. Physical model of heat regenerator.

**1.2. Mathematical Model.** In order to establish the mathematical heat transfer model of honeycomb regenerators, following assumptions were made.

(i) The radiation of smoke and air in the channels is ignored, while convective heat transfer is considered.

(ii) The physical properties of the gas are as same as those of air.

(iii) All physical and thermal parameters of the solid material and gas do not change with temperature.

(iv) Temperatures of hot and cold gas are consistent and stable at the entrance, and do not change with time.

The equations are as follows:

$$\nabla(\rho\vec{U}) = 0, \quad (1)$$

$$\frac{\partial(\rho\vec{U})}{\partial t} + \vec{U}\nabla(\rho\vec{U}) = -\nabla P + \mu\nabla^2\vec{U} + \vec{S}, \quad (2)$$

$$\frac{\partial(\rho T)}{\partial t} + \nabla(\rho\vec{U}T) = \nabla\left(\frac{\lambda}{c_p}\nabla T\right) + \Phi, \quad (3)$$

$$P = \rho RT, \quad (4)$$

$$\frac{\partial(\rho_a T)}{\partial T} = \nabla\left(\frac{\lambda_a}{c_{pa}}\nabla T\right), \quad (5)$$

where  $\rho$  is gas density,  $t$  is time,  $\vec{U}$  is gas velocity vector,  $\mu$  is gas dynamic viscosity,  $P$  is pressure,  $\lambda$  is the thermal conductivity of gas,  $T$  is the temperature,  $c_p$  is the heat capacity,  $\Phi$  is the dissipative function,  $\rho_a$  is the solid density,  $\lambda_a$  is the thermal conductivity of solid, and  $c_{pa}$  is the specific heat of solids.

**1.3. Boundary Conditions.** A regenerating cycle includes heat storing and releasing. During the two stages, velocity at inlet entrance is set as boundary, and exit is set as pressure outlet. Inlet temperatures of the flue gas and the incoming air are 1000 and 27°C, respectively, with the apparent velocity of 0.6 m/s. Switching time is 60 seconds, thus each cycle is 120 s. The initial value of: temperature is 27°C, while velocity and pressure were assumed to attain the initial zero values. The outer surfaces of solid walls are supposed to be adiabatic, while the contact interfaces of the regenerator and gas are treated as the fluid-structure interaction boundary.

**1.4. Calculation Results and Discussion.** In this section, regenerators 2#, 4#, and 6# in Table 1 with porosity of 0.57 are selected. During calculation, three points (the middle one and two edges of the regenerators) are chosen, while the average temperature of them is taken as the temperature of the regenerator.

Figure 2 presents the temperature variation of the selected regenerators with time. It can be seen the temperature change of the hexagon-hole regenerator is more intense than that of the square-hole one, while the round-hole regenerator has the mildest temperature change. Temperature of all regenerators with holes of three different shapes decreases with time, while the temperature difference between them also decreases gradually. At the beginning, the temperature difference between the hexagon- and square-hole regenerators is around 40°C, whereas the respective difference between the hexagon- and round-hole regenerators is 150°C.

**2. Stress Analyses for Honeycomb Ceramic Regenerators.** Based on Fluid Structure Interaction theory, CFX software was employed to calculate the regenerators' thermal stresses. Stress distributions of regenerators with different shapes, porosities and wall thicknesses are studied. Table 2 lists the physical parameters of mullite regenerators.

### 2.1. Stress Analysis with Different Structural Parameters.

**2.1.1. Stress Analysis of Regenerators with Holes of Different Shapes.** Figure 3 presents the stress distribution curves of regenerators with holes of three different shapes. It can be seen that the stress distributions are similar along the length direction. The stresses are greater at the front of the regenerators, and reduce gradually along the length direction, but increase significantly at flue gas outlet. At the ends of the regenerators, thermal stresses are greater and the greatest thermal stresses appear in the high-temperature area.

Table 2

Physical Parameters of Mullite Regenerators [14]

Expansion coefficient ( $\times 10^{-6}, ^\circ\text{C}^{-1}$ )	Elastic modulus (MPa)	Density ( $\text{g}/\text{cm}^3$ )	Coefficient of thermal conductivity [ $\text{W}/(\text{m}\cdot\text{K})$ ]
3.18	128000	2.79	1.68

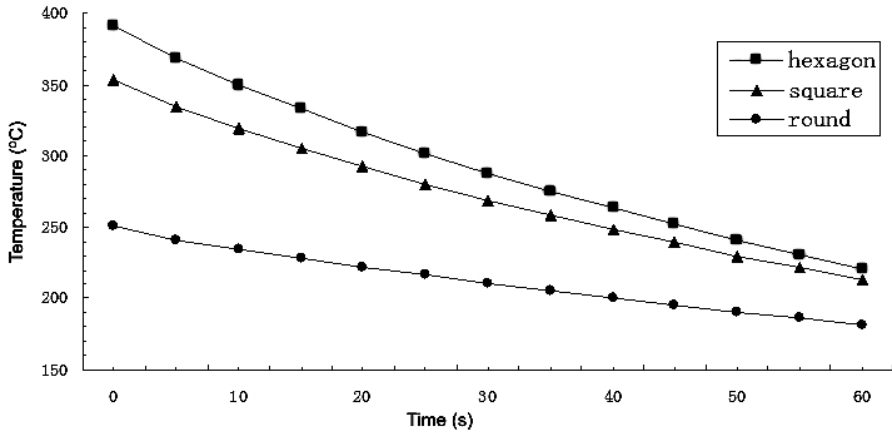


Fig. 2. Temperature distribution of regenerators.

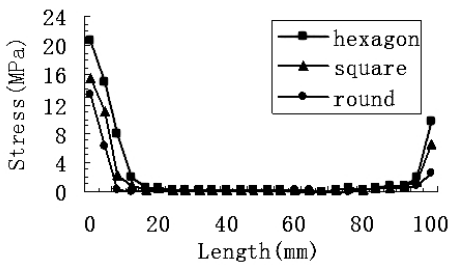


Fig. 3

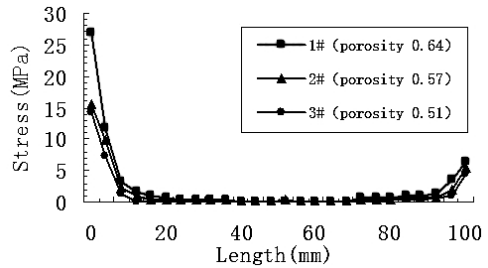


Fig. 4

Fig. 3. Stress distributions of regenerators with holes of three different shapes.

Fig. 4. Stress distributions of square-hole regenerators with different porosities.

Comparing of the stress distributions of the three regenerators, thermal stress of the hexagon-hole regenerator is the greatest, and that of the round-hole regenerator is the smallest. The reason is that with the same porosity and sectional area, hexagon-hole regenerator has the least holes and the highest rate of flow, thus a large temperature difference lead to the highest heat stress. On the other hand, the round-hole regenerator has the greatest number of holes and the lowest thermal stress. This indicates that temperature is the main reason causing thermal stress.

Overall consideration of the heat transfer and thermal shock resistance of the regenerators, square-hole regenerator is more appropriate. To avoid stress concentration caused by the right angle, an arc square hole is designed [15].

2.1.2. *Stress Analysis of Regenerators with Different Porosities.* Two groups of regenerators are chosen for calculation. The first group consists of the 1#, 2#, and 3# square-hole regenerators in Table 1, and the other consists of the 5#, 6#, and 7# round-hole

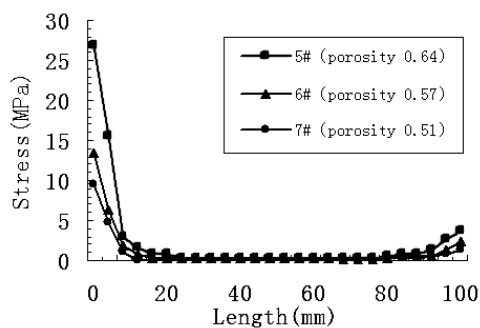


Fig. 5

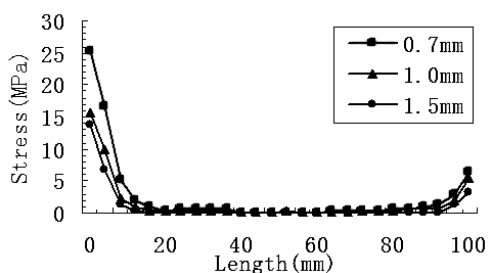


Fig. 6

Fig. 5. Stress distributions of round-hole regenerators with different porosities.

Fig. 6. Stress distributions of regenerators with different wall thickness values.

regenerators. Figures 4 and 5 present the stress distributions of the two groups of regenerators.

As shown in the above two figures, thermal stress increases with porosity. The reason is that the larger the porosity, the stronger the gas liquidity in regenerator channels. Therefore, larger thermal shock is caused by intense temperature changes. Under the premise of ensuring the shock stability of regenerator structures, porosity should be increased as far as possible in the design.

**2.1.3. Stress Analysis of Regenerators with Different Wall Thicknesses.** For this analysis, regenerator 2# in Table 1 is selected. Its thermal stress is analyzed with the wall thickness being 0.7, 1.0, and 1.5 mm, respectively. The stress distribution curves at different wall thicknesses are illustrated in Fig. 6. It can be seen that the stress decreases with the increase of wall thickness. That means the bigger the wall thickness, the better the thermal shock resistance. Yang Gao [16] suggested that the optimal wall thickness is between 0.5 and 1.0 mm considering the heat transfer and resistance of regenerators. In conclusion, wall thickness should be designed with stress, heat transfer and resistance taken into consideration.

## 2.2. Stress Analysis with Different Operational Parameters.

**2.2.1. Stress Analysis with Different Inlet Velocities.** Regenerator 2# in Table 1 is chosen for the study of the influence of inlet velocity. Table 3 lists the three different inlet conditions applied to the regenerator.

Table 3

### Working Conditions

Working condition	Inlet gas velocity (m/s)	Range of temperature (°C)
1	0.6	973
2	0.9	973
3	1.2	973

Stress distributions of the regenerator along the length direction at different velocities are as shown in Fig. 7. It can be seen that the stress increases with velocity. Velocity influences the thermal stress of regenerators mainly through two factors. One is the heat transfer intensity between honeycomb regenerator and gas, and the other is the movement speed in the temperature field. Both heat transfer intensity and movement speed increase with the velocity. Thus, greater thermal shock is caused by intense temperature change. The higher the velocity, the greater the thermal stress.

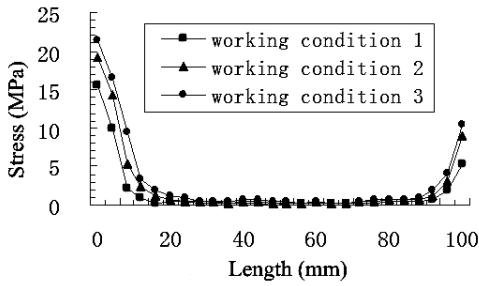


Fig. 7

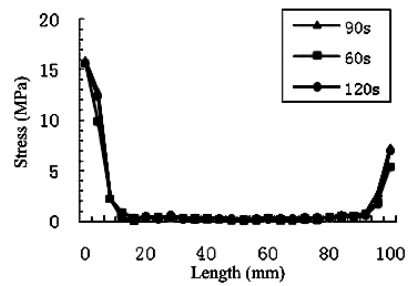


Fig. 8

Fig. 7. Stress distributions at different velocities.

Fig. 8. Stress distributions for different switching times.

Gas velocity not only influences stress of regenerator but also plays a certain role in temperature efficiency and resistance loss of regenerators. With the decrease in velocity, the temperature efficiency will increase, while the resistance loss will decrease. In such conditions, the velocity should be set as low as possible in practice. However, in order to keep sufficient supply of gas, larger cross-sectional area is required for lower inlet velocity, while a larger cross-sectional area implies increases in the volume of regenerator and higher installation and maintenance costs. Therefore, the minimum gas inlet velocity should be limited for the actual situations considered.

*2.2.2. Stress Analysis with Different Switching Times.* Regenerator 2# is selected for the analysis of the effects of different switching times in a cycle on the regenerator's thermal stress. With the same entry conditions and temperature, switching time is set to 60, 90, and 120 s, respectively. Figure 8 presents the stress distributions in situations with different switching times.

As shown in Fig. 8, switching time has a feeble influence on the thermal stress. Even at the ends of the regenerator, stress variation with switching time is not obvious.

**Conclusions.** This paper presents a numerical study on the thermal stress distribution of honeycomb ceramic regenerators with different parameters. The following findings were obtained.

1. Temperature variation of the hexagon-hole regenerator is the most intense, followed by the square-hole regenerator, and that of the round-hole regenerator is the mildest.

2. With the same cross-sectional area, porosity and inlet condition, the hexagon-hole honeycomb ceramic regenerator has the greatest thermal stress, and the round-hole regenerator has the smallest. The stress increases with the increase of porosity, and decreases with the increase of wall thickness.

3. Thermal stress of regenerators increases with the increase of gas inlet velocity. Switching time has a feeble influence on the thermal stress.

**Acknowledgments.** This study was supported by National High Technology Research and Development Program of China (863 Program) (2009AA063202) and Shandong Province Natural Science Fund (ZR2009FQ023, ZR2011EL017).

## Резюме

При роботі ядерного реверс-потокowego реактора керамічні стільникові регенератори зазнають дії термоударного навантаження. За допомогою програмного забезпечення CFX проведено чисельне моделювання епюр температури і температурного напруження керамічних стільникових регенераторів. Досліджено зміну температур у часі для керамічних стільникових регенераторів з отворами різної форми. Проаналізовано епюри температурного напруження регенераторів із різними конструкційними

й експлуатаційними параметрами. Установлено, що температурне напруження керамічного стільникового регенератора залежить від форми отвору, пористості і товщини стінок. Результати даного дослідження є теоретичною базою для оптимізації керамічних стільникових регенераторів.

1. S. Su, A. Beath, H. Guo, and C. Mallett, "An assessment of mine methane mitigation and utilisation technologies," *Prog. Energy Combust. Sci.*, **31**, 123–170 (2005).
2. Z. Gao, Y. Q. Liu, and Z. Q. Gao, "Heat extraction characteristic of embedded heat exchanger in honeycomb ceramic packed bed," *Int. Comm. Heat Mass Transfer*, **39**, 1526–1534 (2012).
3. C. O. Karacan, F. A. Ruiz, M. Cote, and S. Phipps, "Coal mine methane: A review of capture and utilization practices with benefits to mining safety and to greenhouse gas reduction," *Int. J. Coal Geol.*, **86**, 121–156 (2011).
4. Y. P. Cheng, L. Wang, and X. L. Zhang, "Environmental impact of coal mine methane emissions and responding strategies in China," *Int. J. Greenhouse Gas Control*, **5**, 157–166 (2011).
5. I. Karakurt, G. Aydin, and K. Aydiner, "Mine ventilation air methane as a sustainable energy source," *Renew. Sustain. Energy Rev.*, **15**, 1042–1049 (2011).
6. S. Su and J. Agnew, "Catalytic combustion of coal mine ventilation air methane," *Fuel*, **85**, 1201–1210 (2006).
7. Y. Q. Liu, X. C. Chen, R. X. Liu, "Numerical simulation of heat transfer and gas flow characteristics in honeycomb ceramics," *Adv. Mater. Res.*, **156-157**, 984–987 (2011).
8. Y. X. Wang and M. Dong, "Research development of the thermal shock resistance of ceramic honeycomb regenerator," *China Ceram.*, **47**, 1–6 (2011).
9. J. P. Ou, S. J. Jiang, and C.Z. Wu, "Numerical research of the honeycomb ceramic regenerator hole wall stress change characteristics," *Therm. Energy Power Eng.*, **19**, 63–65 (2004).
10. Y. X. Wang, M. Dong, and B. Mu, "Thermal stress research on ceramic honeycomb regenerator," *China Ceram.*, **48**, 39–42 (2012).
11. M. Kalantar and G. Fantozzi, "Thermo-mechanical properties of ceramics: resistance to initiation and propagation of crack in high temperature," *Mater. Sci. Eng.*, **472**, 273–280 (2008).
12. Lin Huo, *Study on How to Improve the Thermal Shock Resistance of Corundum Porcelain Regenerator*, University of Science and Technology, Liaoning (2007).
13. S. X. Song, Xing-Ai, and C. Zh. Huang, "Study development for thermal shock resistance and its mechanisms of ceramics," *Ceram. J.*, **23**, 233–237 (2001).
14. Y. Q. Liu, B. J. Mu, B. Zheng, et al., "Fluid dynamic performance of mullite ceramic honeycomb," *J. Ceram.*, **33**, 162–166 (2012).
15. Y. D. G. Ou, Y. H. Jiang, L. Wei. S. H. Luo Zhu, et al., "Development of honeycomb ceramics thermal storage with low stress," *Industrial Furnace*, **31**, 8–10 (2009).
16. Yang Gao, *Research of Honeycomb Heat Regenerator's Heat Transfer and Resistance Characters*, Chongqing University (2008).

Received 22. 11. 2013